 Related Commentary, page 2855

Deficiency in neuronal TGF-β signaling promotes neurodegeneration and Alzheimer's pathology

Ina Tesseur,[1] Kun Zou,[1] Luke Esposito,[2,3] Frederique Bard,[4] Elisabeth Berber,[1] Judith Van Can,[1] Amy H. Lin,[1] Leslie Crews,[5] Patrick Tremblay,[3] Paul Mathews,[6] Lennart Mucke,[2,3] Eliezer Masliah,[5] and Tony Wyss-Coray[1,7]

[1]Department of Neurology and Neurological Sciences, Stanford University School of Medicine, Stanford, California, USA. [2]Gladstone Institute of Neurological Disease and [3]Department of Neurology, University of California San Francisco, San Francisco, California, USA. [4]Elan Pharmaceuticals Inc., South San Francisco, California, USA. [5]Departments of Neuroscience and Pathology, University of California San Diego, San Diego, California, USA. [6]Center for Dementia Research, New York University School of Medicine, Orangeburg, New York, USA. [7]Geriatric Research, Education, and Clinical Center (GRECC), VA Palo Alto Health Care System, Palo Alto, California, USA.

Alzheimer's disease (AD) is characterized by progressive neurodegeneration and cerebral accumulation of the β-amyloid peptide (Aβ), but it is unknown what makes neurons susceptible to degeneration. We report that the TGF-β type II receptor (TβRII) is mainly expressed by neurons, and that TβRII levels are reduced in human AD brain and correlate with pathological hallmarks of the disease. Reducing neuronal TGF-β signaling in mice resulted in age-dependent neurodegeneration and promoted Aβ accumulation and dendritic loss in a mouse model of AD. In cultured cells, reduced TGF-β signaling caused neuronal degeneration and resulted in increased levels of secreted Aβ and β-secretase–cleaved soluble amyloid precursor protein. These results show that reduced neuronal TGF-β signaling increases age-dependent neurodegeneration and AD-like disease in vivo. Increasing neuronal TGF-β signaling may thus reduce neurodegeneration and be beneficial in AD.

Introduction

Alzheimer's disease (AD) is a progressive neurodegenerative disease that leads to loss of cognitive function in a large number of elderly people. The human AD brain is characterized by the accumulation of β-amyloid peptide (Aβ) in extracellular plaques and hyperphosphorylated tau in intracellular neurofibrillary tangles. In addition, there is degeneration of synapses and dendrites and a progressive loss of neurons involved in memory processes (1). The cause of this degeneration in AD remains unknown, and no effective treatments are available.

Survival of neurons is dependent on extracellular signals from neurotrophic factors and related factors with trophic activity (reviewed in ref. 2). Levels of the neurotrophin nerve growth factor (NGF) and its receptor, tropomyosin receptor kinase A (TRKA), as well as levels of brain-derived neurotrophic factor (BDNF) and its receptor, TRKB, are lower in human AD brains than in nondemented controls (2–5). It was therefore proposed that a deficiency in neurotrophic factor signaling would promote neurodegeneration and cognitive dysfunction in AD, but this hypothesis has not been tested using specific genetic inhibition of neurotrophic factor signaling in a mouse model for AD (reviewed in refs. 2, 6).

Nonstandard abbreviations used: Aβ, β-amyloid peptide; AD, Alzheimer's disease; ALK, activin-like kinase; APP, amyloid precursor protein; BDNF, brain-derived neurotrophic factor; CamKII, calmodulin-dependent kinase II; CTF, C-terminal hAPP fragment; GFAP, glial fibrillary acidic protein; hAPP, human amyloid precursor protein; IDE, insulin-degrading enzyme; MAP2, microtubule-associated protein 2; NeuN, neuronal nuclear protein; NGF, nerve growth factor; Prnp-tTA, prion promoter–driven transactivator tTA; shAPP, soluble hAPP; tetO, tetracycline operator sequences; TRK, tropomyosin receptor kinase; TβRII, TGF-β type II receptor; TβRIIΔk, kinase-deficient TβRII.

Conflict of interest: The authors have declared that no conflict of interest exists.

Citation for this article: *J. Clin. Invest.* **116**:3060–3069 (2006). doi:10.1172/JCI27341.

TGF-βs, which include the isoforms TGF-β1, -2, and -3, are pleiotropic cytokines with important neuroprotective functions (reviewed in refs. 7, 8). TGF-βs are expressed at low levels in the CNS by both neurons and glial cells, and levels of TGF-β1 in particular are increased after injury. TGF-β receptors are expressed throughout the CNS, including adult human neurons (7–9). TGF-βs undergo retrograde transport in neurons and can regulate synaptic growth and differentiation as well as neurotransmitter release in *Drosophila* (reviewed in ref. 10). In *Aplysia*, TGF-β regulates phosphorylation and redistribution of the presynaptic protein synapsin (11). *Tgfb1*$^{-/+}$ mice with 50% reduction in TGF-β1 mRNA levels show increased susceptibility to age- and excitotoxin-induced injury, and *Tgfb1*$^{-/-}$ mice display spontaneous neurodegeneration throughout the brain (12). TGF-βs also synergize with neurotrophins to protect neurons against insults and maintain neuronal health; they may be required for at least some of the trophic effects of NGF, BDNF, neurotrophin 3 (NT-3), and NT-4 (reviewed in ref. 8).

These biological actions of TGF-βs are mediated by a high-affinity transmembrane receptor complex consisting of TGF-β type I receptor activin-like kinase 5 (ALK5) and TGF-β type II receptor (TβRII) serine/threonine kinase receptor subunits. Ligand binding results in receptor phosphorylation and recruitment and phosphorylation of Smad proteins, which translocate to the nucleus and, together with other transcription factors, regulate gene transcription (13). In addition, Smad signaling is modulated by other signaling pathways, including the MAPK, JNK, PKC, and calmodulin-dependent kinase II (CaMKII) pathways (reviewed in ref. 14).

Levels of TGF-βs are increased in human AD brain tissue (15), but decreased in human AD serum (16). Overproduction of TGF-β1 in astrocytes of human amyloid precursor protein (hAPP) transgenic mice reduces overall Aβ accumulation (17), and TGF-βs promote Aβ phagocytosis in rats and in cultured

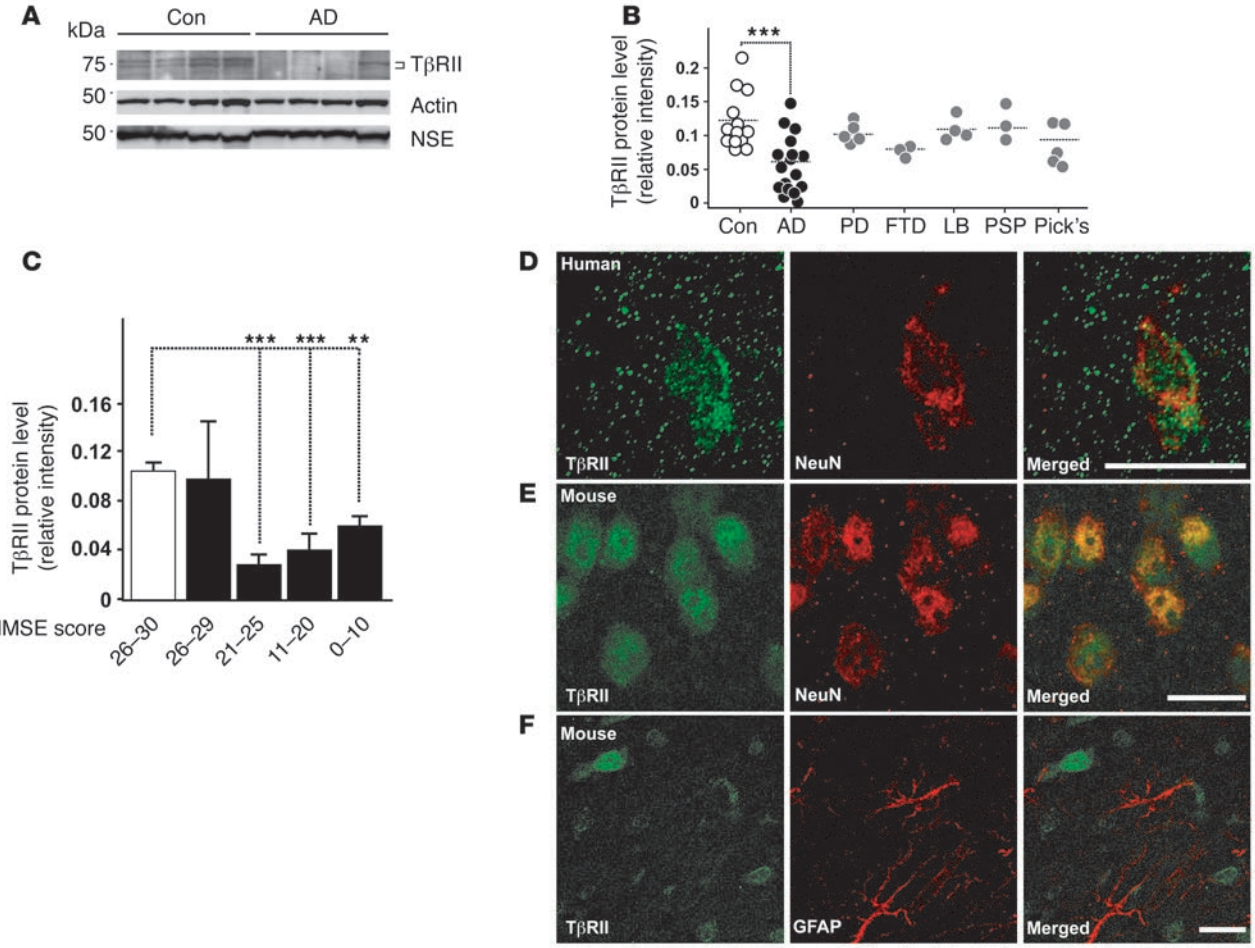

Figure 1

TβRII protein levels are decreased in the human AD brain. (**A**) Representative immunoblots of lysates from AD and age-matched control (Con) parietal corteices probed with antibodies against TβRII, actin, and neuron-specific enolase (NSE). (**B**) TβRII levels of nondemented control, AD, Parkinson's disease (PD), progressive frontotemporal dementia (FTD), lewy body dementia (LB), progressive supranuclear palsy (PSP), and Pick's disease (Pick's) cases were quantified and normalized against protein amounts loaded. Each symbol represents an individual case. (**C**) TβRII protein levels grouped per mini-mental state exam (MMSE) score (white bar, nondemented controls; black bars, AD). (**D** and **E**) TβRII immunofluorescence localized to neurons in the mid-frontal gyrus of the brain from a 69-year-old human (**D**) and the cortex of a 3-month-old wild-type mouse (**E**). (**F**) Little TβRII staining localized to astrocytes in the mouse brain. Scale bars: 10 μm. $^{**}P < 0.05$, $^{***}P < 0.005$; Student's *t* test.

cells (18, 19). Overproduction of TGF-β1 also causes cerebrovascular fibrosis and amyloidosis (17, 20, 21) and has therefore been implicated in cerebral amyloid angiopathy (17, 20–22), a condition frequently associated with AD. Together, these previous findings show that TGF-βs are likely to have beneficial as well as detrimental effects in AD, and since all cells in the CNS express TGF-β receptors, it is unclear which cells are responding to increased or decreased TGF-β levels and what the consequences of signaling are. Also, the important neuroprotective functions of TGF-βs have never to our knowledge been analyzed in models of AD.

Here we studied the importance of TGF-β neurotrophic activity and the possible role of TGF-βs in neurodegeneration and AD. We demonstrate that TGF-β receptor expression was reduced in AD, and via genetic manipulation of neuronal TGF-β signaling we show that reduction of TGF-β signaling in neurons of transgenic mice caused age-dependent neurodegeneration and promoted AD-like pathology in a mouse model for AD.

Results

Decreased TβRII levels in the AD brain. To determine whether TGF-β signaling is altered in human AD brains, we measured levels of TβRII, which is required for transducing TGF-β signals. Western blot analysis of human midfrontal cortex gray matter extracts showed that TβRII levels in human AD brains had on average only half those of nondemented controls (Figure 1, A and B). TβRII protein was identified by 2 different polyclonal antibodies as a doublet of approximately 75 kDa (Figure 1A), consistent with alternative glycosylation forms (23) or the presence of a variant of TβRII containing a 25–amino acid insert in the extracellular domain (24). Comparison of patients and their TβRII levels based on their cognitive function at the last neurological exam showed that TβRII levels were already significantly decreased in AD patients with mild dementia (mini-mental state exam score, 21–25; refs. 25–27) compared with cognitively normal controls (Figure 1C). Levels of neuron-specific enolase were similar in brain extracts of AD and control patients (Figure 1A), suggesting that the decrease in TβRII levels is not merely a consequence of neuron loss

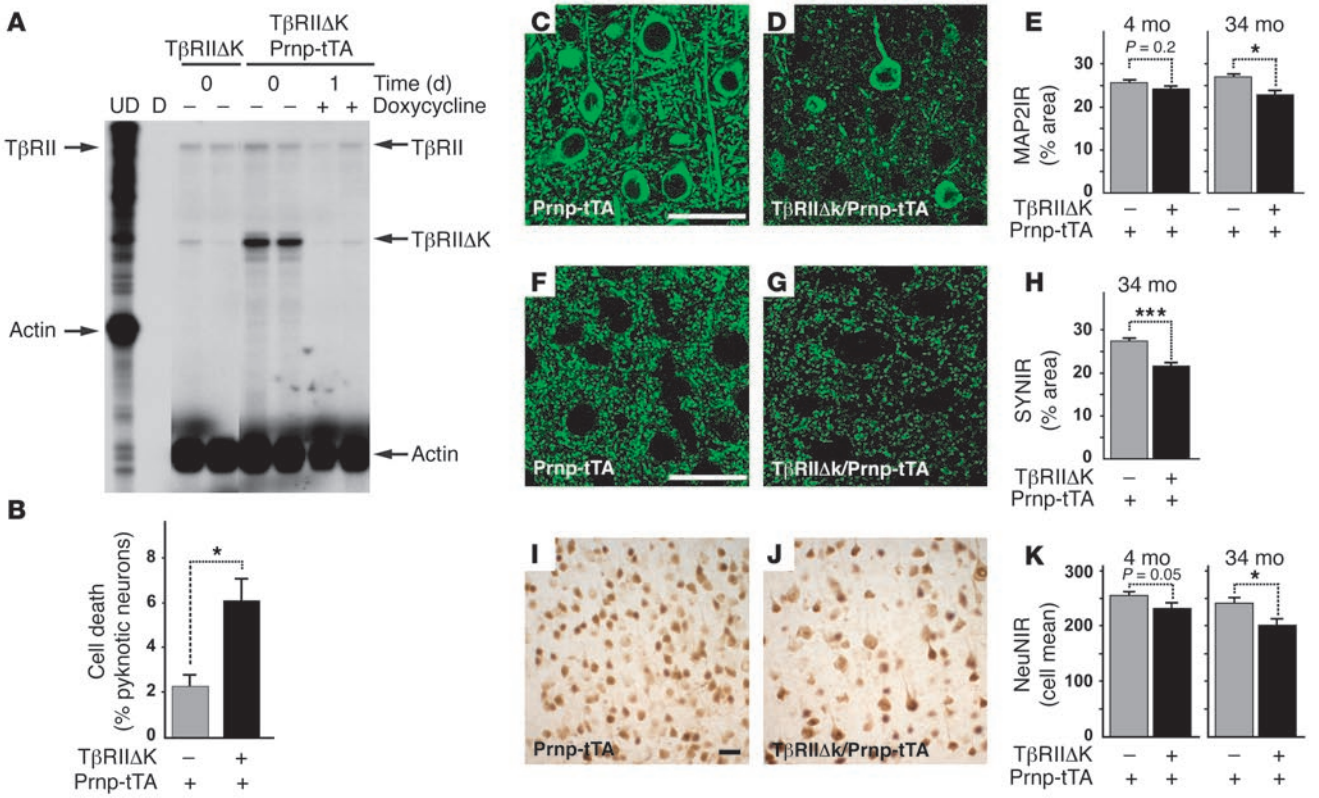

Figure 2

Reduced neuronal TGF-β signaling increases neurodegeneration in vivo. (**A**) RNase protection assay shows TβRIIΔk mRNA expression and inhibition of transgene expression in transgenic mice caused by feeding doxycycline-containing food pellets. Arrows on the left indicate undigested (UD) riboprobes; arrows on the right indicate the corresponding protected fragments. TβRII represents the wild-type receptor. D, digested riboprobe. Each lane represents 1 animal. (**B**) TβRIIΔk-expressing primary neurons show reduced survival in culture. Primary neuron cultures were stained with BODIPY-FL-Fallacidin and Hoechst after 4 days in culture, and the number of viable and dead cells was counted based on the absence or presence of pyknotic nuclei. Data are mean ± SEM of triplicate wells of 3 mice per genotype. (**C**–**K**) Sagittal brain sections of 34-month-old (**C**–**K**) as well as 4-month-old (**E**, **H**, and **K**) *TβRIIΔk/Prnp-tTA* or *Prnp-tTA* mice were immunolabeled for MAP2 (**C**–**E**), synaptophysin (**F**–**H**), and NeuN (**I**–**K**), and percent immunoreactive area (IR) of the neuropil (**C**–**H**) or mean number of labeled cells (**I**–**K**) in the neocortex was determined by confocal microscopy and computer-aided image analysis. Scale bars: 50 μm. Images are examples from cases with clearly visible degeneration. Data are mean ± SEM (n = 5–7 mice per genotype). *P < 0.05, ***P < 0.005; Student's t test.

in AD patients or the agonal state of the disease. Levels of TβRII correlated inversely with measures of neurofibrillary tangle (Braak score; r = –0.59; P < 0.005) and plaque pathology (plaque number/mm^2; r = –0.58; P < 0.003). TβRII levels did not correlate with age (r = 0.05; P = 0.67) or postmortem time to autopsy (r = 0.05; P = 0.71).

To determine whether the decrease in TβRII levels is specific to AD, we also examined TβRII levels in midfrontal cortical gray matter extracts from patients with other dementias or Parkinson's disease. TβRII levels were not significantly decreased in extracts from patients with Parkinson's disease, Pick's disease, progressive supranuclear palsy, lewy body dementia, or frontotemporal dementia compared with controls (Figure 1B), suggesting that the decrease in TβRII may be specific to AD.

To localize TβRII expression in the brain, we stained mouse and human tissue with antibodies against TβRII and cellular markers. Costaining with the neuron-specific marker neuronal nuclear protein (NeuN) showed that TβRII staining localized mainly to neurons in the brains of both healthy humans (Figure 1D) and wild-type mice (Figure 1E). Costaining with the astrocyte-specific marker glial fibrillary acidic protein (GFAP) showed that astrocytes expressed very little TβRII (Figure 1F) compared with neurons (Figure 1, D and E). Based on these results it is conceivable that neuronal TGF-β signaling is impaired in AD.

Decreased neuronal TGF-β signaling in vivo promotes age-related neurodegeneration. Because TGF-βs can be neuroprotective (7, 8) and appear to be essential for maintaining neuronal integrity and survival in vivo (12), we tested whether reduced TGF-β signaling in neurons leads to neurodegeneration in the CNS. We generated transgenic mice expressing kinase-deficient TβRII (TβRIIΔk), which functions as a potent inhibitor of TGF-β signaling and has been used in other transgenic mice to specifically inhibit signaling in pancreatic or skin cells (28, 29). We expressed TβRIIΔk under control of regulatable tetracycline operator sequences (tetO) in neurons by crossing *tetO-TβRIIΔk* mice with previously described *prion promoter–driven transactivator tTA* (*Prnp-tTA*) mice (30). Prnp-tTA mainly restricts tetO-driven transgene expression to neurons in the cortex and hippocampus (30). Double-transgenic *TβRIIΔk/Prnp-tTA* mice expressed TβRIIΔk mRNA in a doxycycline-regulatable manner (Figure 2A). In subsequent experiments, transgene expression was left on (i.e., no doxycycline added) throughout the lifetime of the mice. Primary mixed hippocampal/cortical neurons from *TβRIIΔk/Prnp-tTA* mice showed increased cell death compared with control cultures (Figure 2B), demonstrating

Table 1
Effect of neuronal TGF-β signaling on neurodegeneration and astrocytosis

Age (mo)	Genotype	MAP2 (% area)	Synaptophysin (% area)	NeuN (cell mean)	GFAP (% area)
Neocortex					
4	*Prnp-tTA*	25.6 ± 0.7	ND	254.4 ± 6.0	139.7 ± 5.1
	TβRIIΔk/Prnp-tTA	24.3 ± 0.6	ND	231.5 ± 9.3	132.5 ± 5.4
10	*Prnp-tTA*	25.8 ± 0.9	25.7 ± 1.4	224.0 ± 5.0	154.0 ± 7.8
	TβRIIΔk/Prnp-tTA	24.3 ± 1.1	22.5 ± 1.5	198.0 ± 13.0	170.0 ± 7.3
34	*Prnp-tTA*	26.9 ± 0.7	27.4 ± 0.5	242.7 ± 9.0	152.3 ± 6.5
	TβRIIΔk/Prnp-tTA	22.6 ± 1.1[A]	21.4 ± 0.9[B]	202.4 ± 10.9[A]	181.2 ± 3.6[B]
Hippocampus					
4	*Prnp-tTA*	26.5 ± 0.4	ND	156.1 ± 5.7	232.4 ± 5.3
	TβRIIΔk/Prnp-tTA	25.8 ± 0.5	ND	137.3 ± 6.1	231.7 ± 4.3
10	*Prnp-tTA*	25.6 ± 0.7	25.8 ± 0.9	ND	ND
	TβRIIΔk/Prnp-tTA	24.4 ± 1.0	25.0 ± 0.8	ND	ND
34	*Prnp-tTA*	26.2 ± 1.0	27.6 ± 1.2	ND	255.6 ± 23.3
	TβRIIΔk/Prnp-tTA	24.4 ± 0.5	22.1 ± 1.5[A]	ND	279.1 ± 12.8

Values are mean ± SEM. n = 3–7 mice per group. ND, not done. [A]$P < 0.05$; [B]$P < 0.005$ versus age-matched littermate controls (unpaired Student's t test).

transgene bioactivity as well as a trophic function for TGF-β signaling in neurons. In contrast, the number of glial cells, which represented about 5% of cells in these cultures, was unchanged (data not shown).

Chronic expression of TβRIIΔk in neurons resulted in age-dependent neurodegeneration (Figure 2, C–K, and Table 1). Brains of 34-month-old double-transgenic *TβRIIΔk/Prnp-tTA* mice showed significant decreases in microtubule-associated protein 2–immunoreactive (MAP2-immunoreactive) dendrites (Figure 2, C–E), synaptophysin-immunoreactive presynaptic terminals (Figure 2, F–H), and NeuN-positive neurons (Figure 2, I–K) compared with littermate control mice. Consistent with this neurodegeneration, GFAP immunoreactivity was significantly increased (Table 1). A trend toward neurodegeneration was already observed in the brains of mice at 4 and 10 months of age (Figure 2, E and K, and Table 1).

Decreased neuronal TGF-β signaling in hAPP transgenic mice increases cerebral Aβ accumulation and dendritic degeneration. To study the potential effect of decreased TGF-β signaling in the pathogenesis of AD, we first measured levels of endogenous mouse Aβ in old *TβRIIΔk/Prnp-tTA* and control mice in the absence of familial AD mutations. At 34 months of age, *TβRIIΔk/Prnp-tTA* mice showed a clear trend toward higher endogenous $Aβ_{40}$ and $Aβ_{42}$ levels (as measured by ELISA) compared with *Prnp-tTA* mice, but this did not reach statistical significance ($Aβ_{40}$, *TβRIIΔk/Prnp-tTA,* 377.4 ± 75.7; *Prnp-tTA*, 281.5 ± 13.5; $P = 0.5$; $Aβ_{42}$, *TβRIIΔk/Prnp-tTA,* 233.2 ± 19.3; *Prnp-tTA*, 209.0 ± 31.5; $P = 0.5$). In addition, no Aβ deposits were detected by immunohistochemistry in any of the mice. We therefore crossed a mouse model for AD (*PDGF-hAPP*, line J20; ref. 31) with double-transgenic *TβRIIΔk/Prnp-tTA* mice, and analyzed Aβ deposition and neurodegeneration. Twenty-month-old *hAPP* mice with decreased neuronal TGF-β signaling (*TβRIIΔk/Prnp-tTA/hAPP* mice) showed significantly more Aβ deposition and thioflavin-S–positive amyloid deposits than did *Prnp-tTA/hAPP* littermate controls (Figure 3, A–D, and Table 2). Quantification of Aβ immunostaining demonstrated a 2-fold increase in both total Aβ (anti-$Aβ_{1–5}$ antibody) and $Aβ_{42}$ immunostaining and a 60% increase in the number of thioflavin-S–positive plaques in *TβRIIΔk/Prnp-tTA/hAPP* mice compared with *Prnp-tTA/hAPP* mice (Figure 3, B–D). These histologic findings were confirmed by ELISA measurements of Aβ in hippocampal and cortical brain homogenates. Levels of $Aβ_{1–42}$ and $Aβ_{1–x}$ (which approximates total Aβ) were 2- to 3-fold higher in both brain regions in 20-month-old *TβRIIΔk/Prnp-tTA/hAPP* compared with *Prnp-tTA/hAPP* mice (Table 2). Aβ deposition did not significantly differ at 14 months of age (Figure 3, B and D), and Aβ levels were similar at 2 and 8 months of age (Figure 3, F–H, and Table 2), indicating that age, or time, is an important contributing factor to increased Aβ deposition with decreased neuronal TGF-β signaling. No obvious differences in vascular amyloid were observed at any age between the different groups of mice (data not shown).

To explore the possible cause for this increase in pathology with age, we studied a number of previously described mechanisms that influence Aβ accumulation. There were no significant differences in hAPP protein expression between *TβRIIΔk/Prnp-tTA/hAPP* and *Prnp-tTA/hAPP* mice at 2 (Figure 3I), 14, or 20 months of age, indicating that the increase in Aβ accumulation in *TβRIIΔk/Prnp-tTA/hAPP* mice is not simply due to increased hAPP transgene expression. There were also no significant differences in the expression of insulin-degrading enzyme (IDE; *TβRIIΔk/Prnp-tTA/hAPP*, 0.73 ± 0.08; *Prnp-tTA/hAPP*, 0.88 ± 0.17; $P = 0.5$) and neprilysin (*TβRIIΔk/Prnp-tTA/hAPP*, 0.17 ± 0.02; *Prnp-tTA/hAPP*, 0.17 ± 0.01; $P = 0.8$), 2 Aβ-degrading enzymes involved in cerebral Aβ accumulation in mice (32, 33). There were also no significant differences in apoE levels (*TβRIIΔk/Prnp-tTA/hAPP*, 0.78 ± 0.09; *Prnp-tTA/hAPP*, 0.7 ± 0.05; $P = 0.5$). Lastly, microglial activation, which has been linked to Aβ clearance, was not altered by TβRIIΔk expression as measured by CD68 expression (*TβRIIΔk/Prnp-tTA/hAPP*, 1.24 ± 0.13; *Prnp-tTA/hAPP*, 1.28 ± 0.10; $P = 0.8$). Together, these data indicate that TβRIIΔk expression does not significantly affect hAPP transgene expression or Aβ clearance by neprilysin, IDE, apoE, or activated microglia in 14- to 20-month-old *hAPP* mice and that other mechanisms may be responsible for the development of disease.

One possibility is that reduced TGF-β signaling in neurons might directly alter amyloid precursor protein (APP) processing and lead to increased production of Aβ. While this is easiest studied in cell culture (as described below), we measured the relative levels of major APP cleavage fragments of hAPP in mouse brains using immunoblotting. No significant differences in the levels of α- or β-secretase–cleaved C-terminal hAPP fragments (CTFs) or soluble hAPP (shAPP) were detected in 2- to 14-month-old

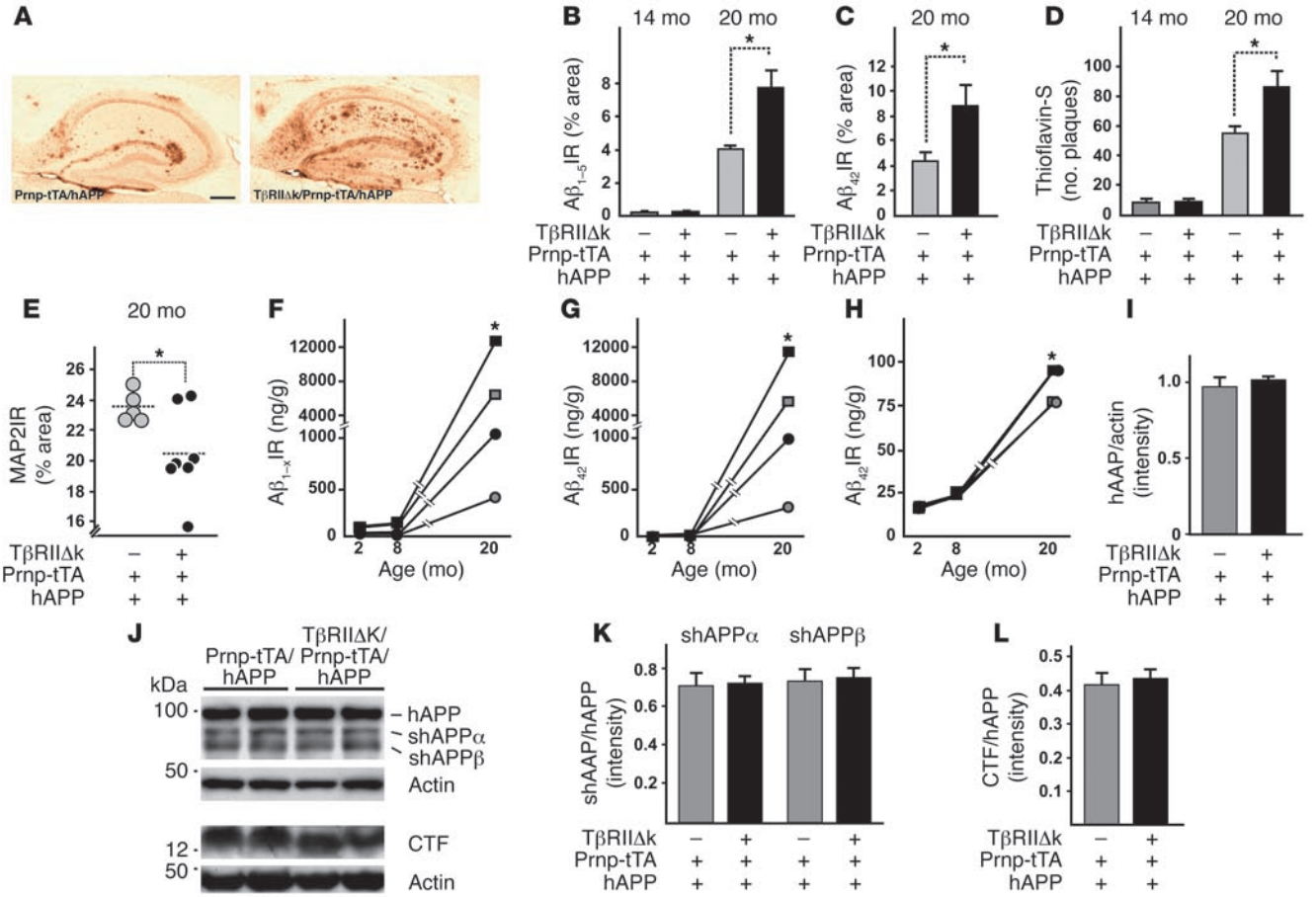

Figure 3

Decreased neuronal TGF-β signaling in old *hAPP* mice increases Aβ levels, amyloid deposition, and dendritic degeneration. (**A**) Representative images of hippocampi of 20-month-old *TβRIIΔk/Prnp-tTA/hAPP* and *Prnp-tTA/hAPP* mice stained with an antibody against $Aβ_{42}$. Scale bar: 500 μm. (**B**–**D**) Quantification of immunoreactive area occupied by staining with antibody against $Aβ_{1–5}$ (**B**), antibody against $Aβ_{42}$ (**C**), and thioflavin-S (**D**) of sagittal sections from 14- and 20-month-old *TβRIIΔk/Prnp-tTA/hAPP* and *Prnp-tTA/hAPP* mice (n = 5–7 mice per genotype). (**E**) Expression of TβRIIΔk in neurons of aged *hAPP* mice reduced MAP2 immunoreactivity in the hippocampus. Sagittal brain sections of 20-month-old mice were stained with MAP2, and percent immunoreactive area of the neuropil was determined by confocal microscopy and computer-aided image analysis. Each symbol represents 1 mouse. (**F**–**H**) Quantification of $Aβ_{1–x}$ (**F**), $Aβ_{42}$ (**G**), and percent $Aβ_{42}$ (**H**) via ELISA in hippocampus (squares) and cortex (circles) of *TβRIIΔk/Prnp-tTA/hAPP* (black symbols) and *Prnp-tTA/hAPP* (gray symbols) mice aged 2, 8, and 20 months (n = 5–7 mice per genotype). Note the cutoff in the y axes. (**I**–**L**) Signal intensities of total APP (**I**), shAPPα and shAPPβ (**K**), and CTFs (**L**) were quantified and normalized against total APP levels (**K** and **L**) or protein amounts loaded (**I**). Representative Western blots (**J**) of cell pellets (hAPP, CTF, and actin) or supernatants (shAPPα and shAPPβ) probed with antibodies against total APP, CTFs, actin, shAPPα, and shAPPβ. *P < 0.05; Student's t test (**B**–**D** and **F**–**H**), Tukey-Kramer test (**E**).

TβRIIΔk/Prnp-tTA/hAPP and *Prnp-tTA/hAPP* mice (Figure 3, J–L). Taken together, these results suggest that reduced TGF-β signaling does not significantly affect APP processing in our mice.

Because *TβRIIΔk/Prnp-tTA* mice showed age-dependent neurodegeneration (Figure 2, C–K), we tested whether the presence of hAPP/Aβ accelerates neuronal damage. Indeed, inhibition of neuronal TGF-β signaling in 20-month-old *Prnp-tTA/hAPP* mice led to a decrease in MAP2-immunoreactive dendrites compared with *hAPP* mice (Figure 3E). In both cortex and hippocampus, MAP2 immunoreactivity correlated inversely with Aβ deposition (data not shown).

Decreased TGF-β signaling promotes neurite degeneration and Aβ production in neuroblastoma cells. To understand how reduced neuronal TGF-β signaling increases neurodegeneration and Aβ accumulation, we studied B103 rat neuroblastoma cells that stably express physiological levels of wild-type hAPP (B103-APPwt) in the absence of endogenous rat APP or APP-like proteins (34).

Transient transfection of B103-APPwt cells with TβRIIΔk, which resulted in up to 90% inhibition of endogenous TGF-β signaling (Figure 4A), caused a characteristic beading of neurites followed by neurite retraction, rounding of the cell body (Figure 4G), and detachment from the plate. The number of neuroblastoma cells with beaded neurites, as well as the number of cells that exhibited rounding, correlated with the level of inhibition of TGF-β signaling (Figure 4, B and C, and data not shown). This reduction in cells with healthy processes was mostly due to induction of cell death, as many affected cells showed pyknotic nuclei (data not shown). Similar results were obtained in mouse neuroblastoma NG108-15 cells (data not shown). Further evidence that TGF-β signaling is required to maintain neuronal integrity was obtained by manipulating downstream com-

Table 2
Effect of neuronal TGF-β signaling on cerebral Aβ accumulation

Age (mo)	Genotype	$A\beta_{1-x}$ (ng/g)	$A\beta_{1-42}$ (ng/g)
Neocortex			
2	*Prnp-tTA/hAPP*	56.7 ± 1.6	9.2 ± 0.6
	TβRIIΔk/Prnp-tTA/hAPP	56.3 ± 3.1	9.8 ± 0.7
8	*Prnp-tTA/hAPP*	51.2 ± 2.9	12.4 ± 1.1
	TβRIIΔk/Prnp-tTA/hAPP	52.9 ± 1.2	13.5 ± 0.8
20	*Prnp-tTA/hAPP*	410.4 ± 70.0	319.8 ± 72.2
	TβRIIΔk/Prnp-tTA/hAPP	1,038.3 ± 311.2[A]	996.4 ± 325.2[B]
Hippocampus			
2	*Prnp-tTA/hAPP*	110.8 ± 5.9	19.0 ± 1.5
	TβRIIΔk/Prnp-tTA/hAPP	99.5 ± 10.2	18.0 ± 1.6
8	*Prnp-tTA/hAPP*	145.6 ± 21.8	30.8 ± 7.0
	TβRIIΔk/Prnp-tTA/hAPP	146.41 ± 26.4	36.5 ± 9.9
20	*Prnp-tTA/hAPP*	6,356.7 ± 244.2	5,622.4 ± 598.5
	TβRIIΔk/Prnp-tTA/hAPP	12,848.7 ± 1735.3[C]	11,437.5 ± 1567.1[C]

Values are mean ± SEM. n = 5–7 mice per group. [A]$P < 0.05$ versus age-matched littermate controls (unpaired Student's t test). [B]$P = 0.08$, [C]$P = 0.06$ versus age-matched littermate controls.

ponents of the TGF-β signaling pathway. Inhibition of the TGF-β type I receptor ALK5 with the kinase inhibitor SB505124 (35) as well as a dominant-negative Smad3 plasmid (36) caused dose-dependent reduction in the number of cells with healthy processes (Figure 4, D and E). Moreover, coexpression of TβRIIΔk with constitutively active Smad3 partially rescued TβRIIΔk-induced degeneration (Figure 4F), and largely restored TGF-β signaling (data not shown). Taken together, these results suggest that TGF-β signaling via Smad transcription factors is necessary to maintain neuronal health and integrity.

To determine whether Aβ production and/or hAPP are required to cause neuritic degeneration after inhibition of TGF-β signaling, we transiently expressed TβRIIΔk in B103 cells stably transfected with a neo plasmid, which lack endogenous APP and hAPP expression (34). Inhibition of 90% of endogenous TGF-β signaling resulted in a phenotype similar to that observed in B103-APPwt cells and decreased the number of cells with healthy processes by 43% (Figure 4C), indicating that Aβ or hAPP are not required for decreased TGF-β signaling to cause neuronal degeneration.

Because TβRIIΔk expression did not affect hAPP expression and did not appear to inhibit Aβ clearance by a number of known mechanisms in vivo, we analyzed whether TβRIIΔk affects APP processing or secretion in B103-APPwt cells transiently transfected with TβRIIΔk. Inhibition of TGF-β signaling resulted in a dose-dependent increase in total Aβ secreted into the culture medium (Figure 5A), causing a 60% increase in Aβ levels under conditions that inhibited TGF-β signaling by 90% (Figure 4A). Similarly, inhibition with the ALK5 inhibitor SB505124 produced a significant increase in secreted Aβ levels (Figure 5B) and shAPP fragments (Figure 5, C and E) and a trend toward increased CTFs (Figure 5, C and F). In contrast, TβRIIΔk expression did not change hAPP production from the CMV-driven transgene in B103-APPwt cells (Figure 5, C and D). Interestingly, the relative increase in shAPPβ was much more prominent than the increase in shAPPα (Figure 5E), suggesting a relative increase in amyloidogenic processing in the absence of TGF-β signaling in these cells.

Discussion

This study provides evidence for a role of endogenous neuronal TGF-β signaling in age-dependent neurodegeneration and Aβ accumulation. We found that TβRII levels were decreased in brain tissue of AD patients, but not in the brain tissue of patients with frontotemporal dementia, lewy body disease, Pick's disease, Parkinson's disease, and progressive supranuclear palsy. Neuronal expression of TβRIIΔk, which lacks signaling activity, resulted in age-dependent synaptic and dendritic degeneration in mice, indicating that neuronal signaling via TβRII is necessary to maintain cellular integrity in vivo. Neuronal expression of TβRIIΔk in an AD mouse model increased Aβ deposition and dendritic degeneration. Our cell culture studies linked the neurodegeneration to Smad signaling, suggesting that at least part of the increase in Aβ deposition may be the result of enhanced amyloidogenic APP processing by neurons with reduced TGF-β signaling.

The observation that TβRII levels were reduced in brain tissue of patients with mild as well as moderate and severe AD (Figure 1) suggests a dysfunction of TGF-β signaling early in the disease. This is consistent with altered expression of TGF-βs in the brain (15) as well as in serum (16). For example, TGF-β1 mRNA levels are increased in human AD brains (20), which may be due to local tissue injury or reflect an attempt to compensate for the reduction in TβRII expression. Alternatively, excess ligand can reduce TβRII levels (37). Interestingly, levels of the neurotrophin receptors TRKA and TRKB are also decreased in AD, specifically in neurons affected by the disease (4, 38, 39). Since TGF-β synergizes with neurotrophins and seems to be required to mediate some of the effects of NGF, BDNF, NT-3, and NT-4 (reviewed in ref. 8), our observation supports the concept of a neurotrophic factor deficiency or signaling dysfunction in AD (6). Neurotrophic signaling deficiency could also be the result of genetic polymorphisms (40), or a frequently found deletion variant of the TGF-β type I receptor ALK5, which reduces TGF-β signaling (41).

We show here that reduced TGF-β signaling in neurons resulted in neurodegeneration (Figure 2) in transgenic mice. TβRIIΔk had prominent effects in cell culture leading to a characteristic beading of neurites followed by neurite retraction and rounding of the cell body similar to the neurodegeneration and formation of varicosities observed by others (42). In *TβRIIΔk* mice, we observed synaptic and dendritic degeneration and possibly neuronal loss as characterized by reduced numbers of NeuN-positive cells. Although the onset of neurodegeneration seems to start at around 4–5 months of age, it progresses with time and may mimic a more subtle decrease in neurotrophic factor signaling, consistent with late onset and slow disease progression in AD. It is possible that in vivo, other neurotrophic factors compensate for the loss in signaling at young ages or that *TβRIIΔk* transgene expression is not high enough to cause significant degeneration at young ages. Importantly, at least in cell culture, hAPP and Aβ were not required to produce neurodegeneration in response to reduced TβRII signaling (Figure 4C).

Besides neurodegeneration, reduced TGF-β signaling also increased amyloid pathology in *hAPP* mice (Figure 3). Lack of neurotrophin expression, systemic production of NGF-neutralizing antibodies, and reduced neuronal TRK signaling were shown to result in neurodegeneration (43–46), but the effect of these manipulations on human Aβ accumulation was not tested. Increased APP expression in a mouse model for Down's syndrome disrupts

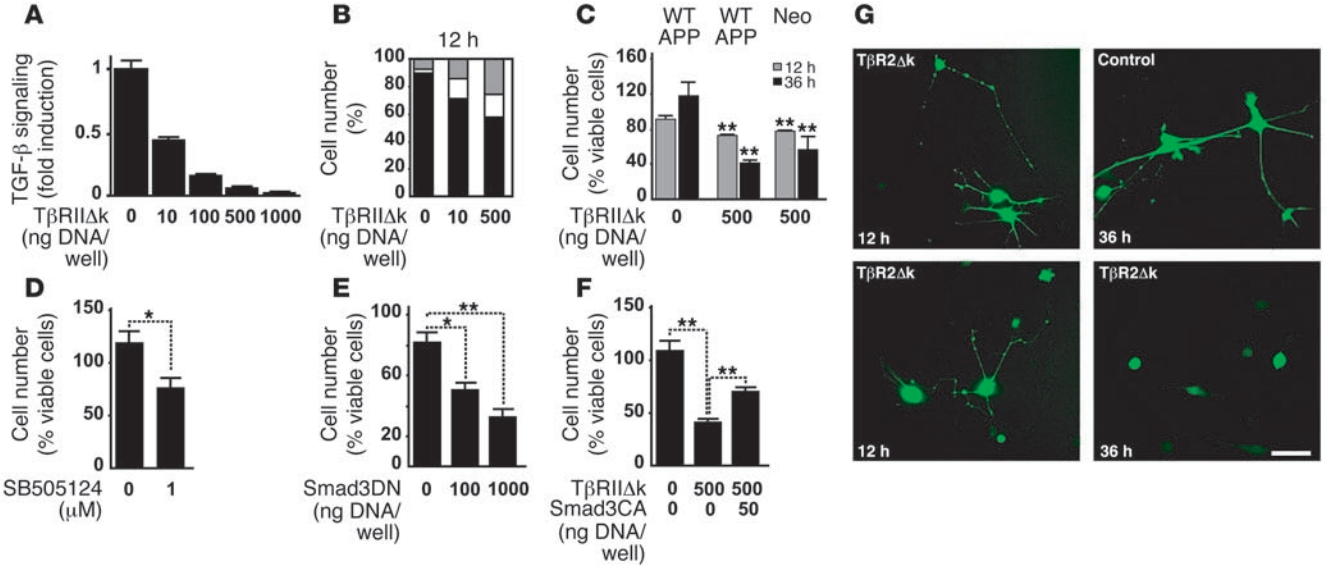

Figure 4

Inhibition of endogenous TGF-β signaling increases neuritic degeneration and Aβ production in neuroblastoma cells. (**A**) Transient transfection of TβRIIΔk and a TGF-β reporter plasmid (p800 luciferase) into B103-APPwt cells dose-dependently inhibited signaling 24 hours after transfection. (**B**) Quantification of the percentage of B103-APPwt cells transiently transfected with TβRIIΔk that showed healthy (black), beaded (white), or no processes (gray) 12 hours after transfection. (**C**) Expression of TβRIIΔk in B103-APPwt (APPwt) or B103 cells lacking APP (neo) significantly reduced the percentage of cells with healthy processes 12 and 36 hours after transfection. (**D**–**F**) Downstream inhibition of TGF-β signaling via treatment with 1 μM SB505124 (**D**) or expression of dominant-negative Smad3 (Smad3DN; **E**) reduced the percentage of cells with healthy processes 36 hours after treatment. (**F**) Expression of constitutively active Smad3 (Smad3CA) partially rescued the phenotype in cells coexpressing TβRIIΔk. (**G**) B103-APPwt cells expressing TβRIIΔk showed beading and retraction of neurites (12 h), followed by rounding up of the cell body (36 h). Control cells were transfected with filler plasmid and GFP. Scale bar: 50 μm. $^{*}P < 0.05$, $^{**}P < 0.01$ versus respective controls; Student's *t* test.

NGF and BDNF transport and results in neurodegeneration, and restoring intracellular BDNF signaling rescues this neuronal cell death (47–49). The TβRII-deficient mice described here carry a well-defined truncated TβRII that has been used successfully in other transgenic mouse models (28, 29) and causes neurodegeneration in cell culture in a Smad3-dependent manner (Figure 4). The increase in amyloid pathology in hAPP mice with decreased TGF-β signaling does not involve increased production of hAPP, decreased levels of the Aβ-degrading enzymes neprilysin and IDE (32, 33), or changes in apoE expression or microglial activation. Although we cannot exclude an effect on Aβ clearance due to effects on other known pathways (50, 51), the results of our studies in neuroblastoma cells suggest that TGF-β signaling deficiency may promote Aβ deposition at least in part by increasing amyloidogenic hAPP processing. Thus, expression of TβRIIΔk or treatment with a TGF-β type I receptor kinase inhibitor, both of which cause neurodegeneration, increased the levels of Aβ in cell culture supernatant (Figure 5, A and B). Although inhibition of TGF-β signaling resulted in increased Aβ levels as well as shAPP fragments and CTFs in cultured neurons (Figure 5), this was not observed in vivo (Figure 3). This discrepancy could be due to acute inhibition in cell culture versus chronic inhibition in vivo. Also, the ALK5 inhibitor seems to slightly inhibit ALK4 and ALK7 receptors, which are involved in activin and nodal signaling (35). Furthermore, it is possible that the effects in vivo are much more subtle than in cell culture, and because the APP mutation in the *hAPP* mice already shifts APP processing toward the amyloidogenic pathway, we would only observe a clear difference with age. The precise mechanism by which reduced TGF-β signaling alters APP processing is under investigation, but we speculate that similar stress pathways, known to increase Aβ production in other systems (reviewed in ref. 52), may be involved.

In summary, we present evidence that neuronal TGF-β signaling is impaired in AD and that reduced neuronal TGF-β signaling via Smad transcription factors can lead to age-dependent and Aβ-induced neurodegeneration in experimental models. Reduced TGF-β signaling may deprive neurons of their trophic support and appears to promote amyloidogenic APP processing. Increasing neuronal TGF-β signaling could provide a potential protective strategy against age-related neurodegeneration and AD.

Methods

Mice and tissue collection. Transgenic mice expressing hAPP under control of the platelet-derived growth factor B chain promoter on the C57BL/6 genetic background with an alternatively spliced minigene that encodes hAPP695, hAPP751, and hAPP770 bearing the amyloidogenic K670M/N671L and V717F mutations, were described (*hAPP* mice, line J20; ref. 31). Transgenic mice expressing a truncated TβRIIΔk under control of tetO regulatory sequences (*tetO-TβRIIΔk* mice) were generated using standard procedures. Briefly, a 600-bp Klenow-filled *Sfi*I/*Eco*RI fragment from CMV-TβRIIΔk (plasmid XF120; obtained from R. Derynck, UCSF, San Francisco, California, USA; ref. 53) was subcloned into pGEM11Z, excised with *Eco*RI/*Xba*I, ligated into pUHG16-3 (which contains heptamerized tet-operators flanked by a minimal CMV promoter; ref. 54), and microinjected into fertilized embryos. *Prnp-tTA* mice expressing tTA mostly in neurons have been described previously (30) and were crossed with *tetO-TβRIIΔk* mice to induce neuronal expression of TβRIIΔk. *TβRIIΔk/Prnp-tTA* mice were crossed with *hAPP* mice for 2 generations to generate triple-transgenic *TβRIIΔk/Prnp-tTA/hAPP* mice heterozygous for the respective transgenes. *Prnp-tTA/hAPP* transgenic litter-

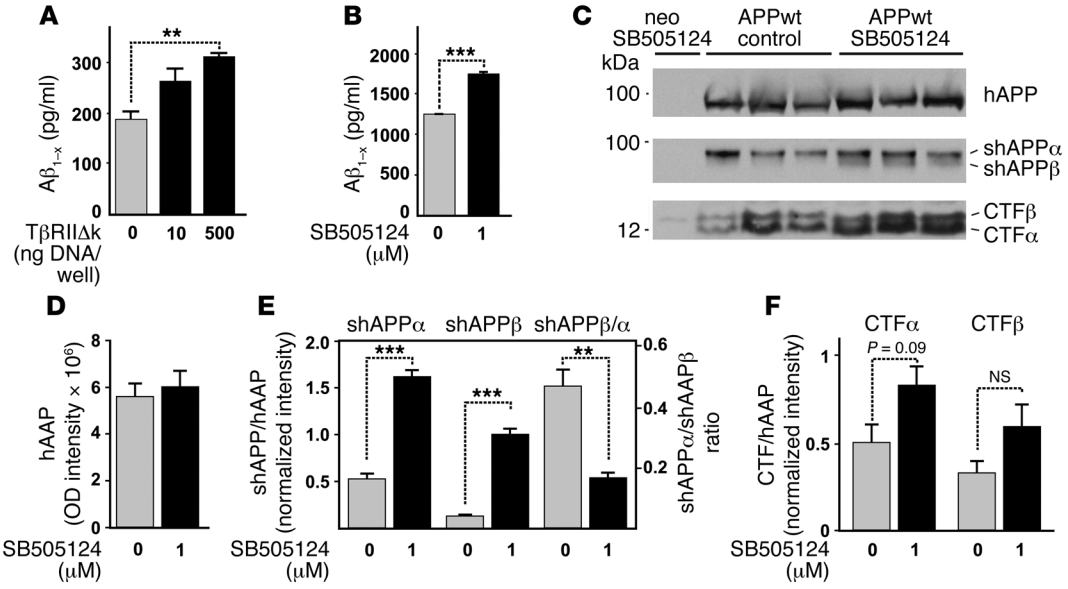

Figure 5

Inhibition of neuronal TGF-β signaling increases Aβ, shAPP and CTF in neuroblastoma cells. (**A** and **B**) B103-APPwt cells were transiently transfected with TβRIIΔk and GFP and sorted via fluorescence-activated cell sorting (**A**) or treated with 1 μM SB505124 to inhibit ALK5 signaling (**B**). Total secreted Aβ was measured via ELISA 5 days after treatment. (**C**) Representative Western blots of cell pellets (hAPP, CTFα, CTFβ) or supernatants (shAPPα, shAPPβ) of B103-APPwt cells or B103 cells lacking APP treated with 0 or 1 μM SB505124 and probed with antibodies against total hAPP, CTFα, CTFβ, shAPPα, and shAPPβ. (**D**–**F**) Signal intensities of total hAPP (**D**), shAPPα and shAPPβ (**E**), and CTFα and CTFβ (**F**) were quantified and normalized against hAPP levels (**E** and **F**), and the ratio between shAPPα and shAPPβ was calculated (**E**). Data are mean ± SEM of triplicate wells of 1 representative experiment. $^{**}P < 0.01$, $^{***}P < 0.001$; Student's *t* test.

mates served as controls. To confirm that the tetO-TβRIIΔk transgene can be regulated, doxycycline-containing food pellets were fed ad libitum to mice used for analysis of transgene expression (doxycycline pellets; 200 mg/kg; Bio-serv). Mice used to analyze age-related neurodegeneration and amyloid deposition did not receive doxycycline. All mice were on the C57BL/6 genetic background, heterozygous for any of the transgenes, and genotyped by PCR using appropriate oligonucleotide primers. Mice were kept under a 12-hour light/12-hour dark cycle with free access to sterile food and acidified water and used in accordance with institutional guidelines.

Mice were flush-perfused transcardially with phosphate buffer and, one hemibrain was fixed for 48 hours in 4% paraformaldehyde and equilibrated in 30% sucrose for histologic processing. The other hemibrain was dissected into hippocampus, cortex, thalamus, and brainstem, snap-frozen in isopentane on dry ice, and stored at –80°C until use.

All animal care and use was in accordance with institutional guidelines and approved by the Palo Alto VA Committee on Animal Research.

Human postmortem brain tissue. Midfrontal cortex tissue samples form neurologically unimpaired subjects ($n = 11$) and from subjects with AD ($n = 18$) were obtained from the Department of Pathology, University of California, San Diego. Diagnosis of AD was confirmed by pathological and clinical criteria. Tissue was frozen at autopsy and stored at –80°C until use. The average age of subjects was 80.5 ± 2.4 years in the AD group and 79.0 ± 9.0 years in the control group ($P = 0.8$). Average postmortem delay was 9.6 hours and was not significantly different between groups. One AD case and 3 control cases were excluded from the analysis due to protein degradation of the sample as assessed by coomassie staining of SDS-PAGE gels.

Cells and tissue culture. B103 rat neuroblastoma cells stably transfected with human wild-type APP or a neo plasmid (34) and NG108-15 neuroblastoma cells (ATCC; HB-12317) were cultured in DMEM supplemented with 10% FBS and 5% heat-inactivated horse serum. Cells were seeded at 50,000 cells/well in 12-well plates and transiently transfected with plasmids encoding for TβRIIΔk, GFP (Invitrogen), pBluescript (Invitrogen), PAI-1-luciferase (55) or SBE-luciferase (56), and constitutively active Smad3 (36) or dominant-negative Smad3 (36) using Superfect (QIAGEN) according to the manufacturer's instructions. GFP-expressing cells were counted after 12, 36, and 60 hours in culture. Luciferase activity was measured after 24 hours with a LMax plate photometer (Molecular Devices) using a Luciferase Assay System (Promega) according to the manufacturer's instructions. Solid anhydrous SB-505124 (Tocris Bioscience) was reconstituted in DMSO to a concentration of 1 mM and further diluted to 1 μM immediately prior to use.

Postnatal primary neuronal and astroglial cell cultures. Mixed hippocampal-neocortical primary neuronal cultures and primary astroglial cultures were prepared from P1 and P3 mice, respectively, generated through matings between heterozygous *Prnp-tTA* and *tetO-TβRIIΔk* mice as described previously (12). Primary neurons were used at 2 or 4 days in culture. After fixation in 4% paraformaldehyde, cells were labeled with BODIPY-FL-phallacidin (Invitrogen) to stain the actin cytoskeleton according to the manufacturer's instructions. Cultures were costained with Hoechst 33342 (Invitrogen) to label DNA and examined with an Olympus IX70 inverted fluorescence microscope connected to a CoolSNAP HQ camera (Photometrics). Images were processed and analyzed using Metamorph Imaging software (version 6.1r1; Universal Imaging Corp., Molecular Devices) and Adobe Photoshop version 6.0.1. The experimenter was blinded to the genotypes of the mice.

Protein extraction and immunoblotting. Human tissue was dissected into gray and white matter, and gray matter was lysed in extraction buffer consisting of 20 mM Tris-HCl (pH 7.4), 10 mM EDTA, 10 mM EGTA, 1% sodium-dodecylsulphate, and 1 tablet complete proteinase inhibitor (Roche Diagnostics) per 50 ml extraction buffer. Equal amounts of protein were subjected to SDS-PAGE under reducing conditions in 3%–8% NuPAGE Novex gels (Invitrogen), transferred to nitrocellulose membranes (Bio-Rad), and

probed with antibodies against TβRII (Upstate USA Inc.; 4 mg/ml). Mice were flush-perfused, and brains were dissected into hippocampus and cortex and homogenized in a buffer containing 1 mM HEPES, pH 8.8; 5 mM benzamidine; 2 mM β-mercaptoethanol; 3 mM EDTA; 0.5 mM magnesiumsulphate; and 0.05% sodiumazide. Pellets were further homogenized in equal volumes of RIPA buffer, and proteins were separated on 4%–12% Bis-Tris NuPAGE Novex gels (Invitrogen). Supernatants were probed with antibodies against the N-terminal (diluted 1:1,000, 8E5; Elan) and pellets with antibodies against the C-terminal (diluted 1:1,000; kindly provided by T. Golde, Mayo Clinic College of Medicine, Jacksonville, Florida, USA) fragments of APP. To adjust for loading differences, blots were stripped and reprobed with an antibody against actin (diluted 1:250; Chemicon International), and gels were stained with GelCode Blue Stain Reagent (Pierce) to check for protein degradation. To confirm the loading of equal amounts of neurons, blots were stripped and reprobed with an antibody against neuron-specific enolase (diluted 1:1,000; Lab Vision Corp.). Binding of secondary antibodies was visualized by ECL (Amersham Biosciences), and signal intensities were quantified with Metamorph Imaging software. Relative receptor levels were calculated by normalizing to actin levels.

Fluorescence-activated cell sorting. Cells were transiently transfected with TβRIIΔk, GFP and pBluescript. Twelve hours after transfection, cells were dissociated, spun, resuspended in growth medium, and filtered through a 40-μm nylon mesh. Sorting and analysis were carried out on a FACSVantage SE flow cytometer (BD). Dead cells and GFP-negative cells were excluded by gating on forward and side scatter. Mock-transfected cells were used to set background fluorescence. Viable GFP-positive cells were sorted into growth medium and immediately replated at 70% confluency in 12-well plates. Twelve hours after replating, cells were incubated with serum-free neurobasal medium supplemented with N2 for 5–7 days. Supernatants and pellets were collected separately for Aβ and APP measurements, respectively.

RNA extraction and analysis. Total RNA from snap-frozen hemibrains was isolated with TRI reagent (Molecular Research Center Inc.) and analyzed by solution hybridization RNase protection assay as previously described (17). The [^{32}P]-antisense riboprobes used to identify specific mRNAs were murine β-actin (nt 480–559 protected; GenBank accession no. M18194) and TβRII (nt 425–828 protected; GenBank accession no. S69114), which protects a shorter segment of mRNA in TβRIIΔk (nt 425–601 protected).

Aβ ELISA. Snap-frozen hippocampi and cortices were homogenized in 5 M guanidine-HCl buffer, and Aβ peptides were quantified by ELISA as described previously (17). Cell culture conditioned media were centrifuged to pellet dead cells and stored at –80°C. Samples were thawed on ice immediately prior to use.

Immunohistochemistry. Fixed hemibrains were equilibrated in 30% sucrose in phosphate-buffered saline and cut into 40-μm sections with a freezing microtome (Leica Microsystems). Thioflavin-S staining was carried out as described previously (17). Microtome sections were immunoperoxidase labeled with a VECTASTAIN Elite ABC Kit (Vector Laboratories) using anti-Aβ_{1-5} (1 μg/ml, 3D6; Elan), anti-Aβ_{1-42} (1 μg/ml, 21F12; Elan), biotinylated donkey anti-mouse (diluted 1:3,000; Vector Laboratories), and DAB (Sigma-Aldrich). The percentage area of the hippocampus covered by 3D6 or 21F12 immunoreactivity or by thioflavin-S staining was determined with Metamorph Imaging software using an Olympus microscope connected to a CoolSNAP HQ camera. For each mouse, 3–4 sections were analyzed, and the average was used to calculate group means. Similarly, brain sections were labeled with CD68 to detect activated microglia (diluted 1:10; Serotec), GFAP (diluted 1:1,000; Dako) to detect reactive astrocytes, and NeuN (diluted 1:1,000; Chemicon International) to detect neurodegeneration and relative immunoreactivity, and mean cell numbers were quantified using the previously described selector method (57).

For MAP2-immunoreactive postsynaptic dendrites and synaptophysin-immunoreactive presynaptic terminals, brain sections were labeled with anti-MAP2 (1 μg/ml; Roche Diagnostics) and anti-Syn (diluted 1:800; Roche Diagnostics), respectively. Secondary antibody FITC-conjugated horse anti-mouse IgG (diluted 1:75; Vector Laboratories) was added and sections were imaged with confocal microscopy via the selector method (57). Briefly, counts per unit area were obtained by computer-aided image analysis morphometry in 2–4 sections per mouse at 3 images per section, and digitized images 0.5 μm thick were thresholded for immunolabeled area. The area occupied by MAP2- or synaptophysin-immunoreactive terminals of defined signal intensity were quantified and expressed as a percentage of the total image area (57, 58). This approach for the quantitative assessment of neurodegeneration has been validated in various experimental models of neurodegeneration (59–61) and in diseased human brain (62).

For TβRII, cryosections were fixed in 100% methanol and stained with antibodies against TβRII (4 μg/ml; Upstate USA Inc.), followed by postfixation in 4% paraformaldehyde and labeling with antibodies against NeuN (diluted 1:1,000; Chemicon International) or GFAP (diluted 1:1,000; Santa Cruz Biotechnology Inc.).

Statistics. Differences between 2 means were assessed by Mann-Whitney *U* or unpaired 2-tailed Student's *t* test for nonparametric or parametric data, respectively. Differences among multiple means of data with parametric distribution were assessed by ANOVA followed by Tukey-Kramer post-hoc test. All statistical analyses were performed with StatView version 5.0 software (SAS). For histochemical and immunohistochemical studies, brain sections were coded, and codes were not broken until analyses were complete. *P* values of 0.05 or less were considered to be significant.

Acknowledgments

We would like to thank Stanley B. Prusiner (University of California, San Francisco) for providing us with the *Prnp-tTA* mice. We thank L. Head (University of California Irvine, Irvine, California, USA) for providing us with Parkinson's disease, Pick's disease, Progressive Supranuclear Palsy, Lewy Body dementia, and Frontotemperal dementia brain tissue and T. Golde (Mayo Clinic College of Medicine, Jacksonville, Florida, USA) for providing us with the CTF-specific APP antibody. This work was supported by NIH grants AG20603 and NS40994 (T. Wyss-Coray), the John Douglas French Alzheimer's Foundation (I. Tesseur) and the Alzheimer's Association (I. Tesseur and T. Wyss-Coray).

Received for publication November 7, 2005, and accepted in revised form August 1, 2006.

Address correspondence to: Tony Wyss-Coray, Stanford University Medical Center, Rm-A343, Stanford, California 94305-5235, USA. Phone: (650) 852-3220; Fax: (650) 849-0434; E-mail: twc@stanford.edu.

Patrick Tremblay's present address is: Neurochem Inc., Laval, Quebec, Canada.

1. Selkoe, D.J. 2001. Alzheimer's disease: genes, proteins, and therapy. *Physiol. Rev.* **81**:741–766.
2. Connor, B., and Dragunow, M. 1998. The role of neuronal growth factors in neurodegenerative disorders of the human brain. *Brain Res. Brain Res. Rev.* **27**:1–39.
3. Murer, M.G., Yan, Q., and Raisman-Vozari, R. 2001. Brain-derived neurotrophic factor in the control human brain, and in Alzheimer's disease and Parkinson's disease. *Prog. Neurobiol.* **63**:71–124.
4. Allen, S.J., Wilcock, G.K., and Dawbarn, D. 1999. Profound and selective loss of catalytic TrkB immunoreactivity in Alzheimer's disease. *Biochem. Biophys. Res. Commun.* **264**:648–651.
5. Ferrer, I., et al. 1999. BDNF and full-length and

truncated TrkB expression in Alzheimer disease. Implications in therapeutic strategies. *J. Neuropathol. Exp. Neurol.* **58**:729–739.
6. Hefti, F. 1997. Pharmacology of neurotrophic factors. *Annu. Rev. Pharmacol. Toxicol.* **37**:239–267.
7. Flanders, K.C., Ren, R.F., and Lippa, C.F. 1998. Transforming growth factor–βs in neurodegenerative disease. *Prog. Neurobiol.* **54**:71–85.
8. Unsicker, K., and Krieglstein, K. 2002. TGF-betas and their roles in the regulation of neuron survival. *Adv. Exp. Med. Biol.* **513**:353–374.
9. Lippa, C.F., Flanders, K.C., Kim, E.S., and Croul, S. 1998. TGF-beta receptors-I and -II immunoexpression in Alzheimer's disease: a comparison with aging and progressive supranuclear palsy. *Neurobiol. Aging.* **19**:527–533.
10. Sanyal, S., Kim, S.M., and Ramaswami, M. 2004. Retrograde regulation in the CNS; neuron-specific interpretations of tgf-Beta signaling. *Neuron.* **41**:845–848.
11. Chin, J., Angers, A., Cleary, L.J., Eskin, A., and Byrne, J.H. 2002. Transforming growth factor β1 alters synapsin distribution and modulates synaptic depression in *Aplysia*. *J. Neurosci.* **22**:1–6.
12. Brionne, T.C., Tesseur, I., Masliah, E., and Wyss-Coray, T. 2003. Loss of TGF-beta1 leads to increased neuronal cell death and microgliosis in mouse brain. *Neuron.* **40**:1133–1145.
13. Dennler, S., Goumans, M.-J., and Dijke, P.T. 2002. Transforming growth factor β signal transduction. *J. Leukoc. Biol.* **71**:731–740.
14. Feng, X.H., and Derynck, R. 2005. Specificity and versatility in TGF-beta signaling through smads. *Annu. Rev. Cell Dev. Biol.* **21**:659–693.
15. Flanders, K.C., Lippa, C.F., Smith, T.W., Pollen, D.A., and Sporn, M.B. 1995. Altered expression of transforming growth factor-β in Alzheimer's disease. *Neurology.* **45**:1561–1569.
16. De Servi, B., La Porta, C.A.M., Bontempelli, M., and Comolli, R. 2002. Decrease of TGF-β1 plasma levels and increase of nitric oxide synthase activity in leukocytes as potential biomarkers of Alzheimer's disease. *Exp. Gerontol.* **37**:813–821.
17. Wyss-Coray, T., et al. 2001. TGF-β1 promotes microglial amyloid-β clearance and reduces plaque burden in transgenic mice. *Nat. Med.* **7**:612–618.
18. Frautschy, S.A., Cole, G.M., and Baird, A. 1992. Phagocytosis and deposition of vascular β-amyloid in rat brains injected with Alzheimer β-amyloid. *Am. J. Pathol.* **140**:1389–1399.
19. Magnus, T., Chan, A., Linker, R.A., Toyka, K.V., and Gold, R. 2002. Astrocytes are less efficient in the removal of apoptotic lymphocytes than microglia cells: implications for the role of glial cells in the inflamed central nervous system. *J. Neuropathol. Exp. Neurol.* **61**:760–766.
20. Wyss-Coray, T., et al. 1997. Amyloidogenic role of cytokine TGF-β1 in transgenic mice and Alzheimer's disease. *Nature.* **389**:603–606.
21. Ueberham, U., et al. 2005. Inducible neuronal expression of transgenic TGF-beta1 in vivo: dissection of short-term and long-term effects. *Eur. J. Neurosci.* **22**:50–64.
22. Grammas, P., and Ovase, R. 2002. Cerebrovascular transforming growth factor-β contributes to inflammation in the Alzheimer's disease brain. *Am. J. Pathol.* **160**:1583–1587.
23. Lin, H.Y., et al. 1995. The soluble exoplasmic domain of the type II transforming growth factor (TGF)-beta receptor. A heterogeneously glycosylated protein with high affinity and selectivity for TGF-beta ligands. *J. Biol. Chem.* **270**:2747–2754.
24. Rotzer, D., et al. 2001. Type III TGF-beta receptor-independent signalling of TGF-beta2 via TbetaRII-B, an alternatively spliced TGF-beta type II receptor. *EMBO J.* **20**:480–490.
25. Folstein, M.F., Folstein, S.E., and McHugh, P.R. 1975. "Mini-mental state". A practical method for grading the cognitive state of patients for the clinician. *J. Psychiatr. Res.* **12**:189–198.
26. Neale, R., Brayne, C., and Johnson, A.L. 2001. Cognition and survival: an exploration in a large multicentre study of the population aged 65 years and over. *Int. J. Epidemiol.* **30**:1383–1388.
27. Perneczky, R., et al. 2006. Mapping scores onto stages: mini-mental state examination and clinical dementia rating. *Am. J. Geriatr. Psychiatry.* **14**:139–144.
28. Böttinger, E.P., et al. 1997. Expression of a dominant-negative mutant TGF-β type II receptor in transgenic mice reveals essential roles for TGF-β in regulation of growth and differentiation in the exocrine pancreas. *EMBO J.* **16**:2621–2633.
29. Wang, X.J., et al. 1997. Expression of a dominant-negative type II transforming growth factor β (TGF-β) receptor in the epidermis of transgenic mice blocks TGF-β-mediated growth inhibition. *Proc. Natl. Acad. Sci. U. S. A.* **94**:2386–2391.
30. Tremblay, P., et al. 1998. Doxycycline control of prion protein transgene expression modulates prion disease in mice. *Proc. Natl. Acad. Sci. U. S. A.* **95**:12580–12585.
31. Mucke, L., et al. 2000. High-level neuronal expression of $A\beta_{1-42}$ in wild-type human amyloid protein precursor transgenic mice: synaptotoxicity without plaque formation. *J. Neurosci.* **20**:4050–4058.
32. Farris, W., et al. 2003. Insulin-degrading enzyme regulates the levels of insulin, amyloid beta-protein, and the beta-amyloid precursor protein intracellular domain in vivo. *Proc. Natl. Acad. Sci. U. S. A.* **100**:4162–4167.
33. Iwata, N., et al. 2001. Metabolic regulation of brain Abeta by neprilysin. *Science.* **292**:1550–1552.
34. Esposito, L., Gan, L., Yu, G.Q., Essrich, C., and Mucke, L. 2004. Intracellularly generated amyloid-beta peptide counteracts the antiapoptotic function of its precursor protein and primes proapoptotic pathways for activation by other insults in neuroblastoma cells. *J. Neurochem.* **91**:1260–1274.
35. DaCosta Byfield, S., Major, C., Laping, N.J., and Roberts, A.B. 2004. SB-505124 is a selective inhibitor of transforming growth factor-beta type I receptors ALK4, ALK5, and ALK7. *Mol. Pharmacol.* **65**:744–752.
36. Liu, X., et al. 1997. Transforming growth factor beta-induced phosphorylation of Smad3 is required for growth inhibition and transcriptional induction in epithelial cells. *Proc. Natl. Acad. Sci. U. S. A.* **94**:10669–10674.
37. Gebken, J., et al. 1999. Ligand-induced downregulation of receptors for TGF-beta in human osteoblast-like cells from adult donors. *J. Endocrinol.* **161**:503–510.
38. Counts, S.E., et al. 2004. Reduction of cortical TrkA but not p75(NTR) protein in early-stage Alzheimer's disease. *Ann. Neurol.* **56**:520–531.
39. Mufson, E.J., et al. 2000. Loss of nucleus basalis neurons containing trkA immunoreactivity in individuals with mild cognitive impairment and early Alzheimer's disease. *J. Comp. Neurol.* **427**:19–30.
40. Bertram, L., McQueen, M., Mullin, K., Blacker, D., and Tanzi, R. The AlzGene database. Alzheimer Research Forum. http://www.alzgene.org.
41. Chen, Y.X., et al. 1995. Molecular detection of pre-ATL state among healthy HTLV-1 carriers in an endemic area of Japan. *Int. J. Cancer.* **60**:798–801.
42. Ferreira, A., Lu, Q., Orecchio, L., and Kosik, K.S. 1997. Selective phosphorylation of adult tau isoforms in mature hippocampal neurons exposed to fibrillar A beta. *Mol. Cell. Neurosci.* **9**:220–234.
43. Capsoni, S., et al. 2000. Alzheimer-like neurodegeneration in aged antinerve growth factor transgenic mice. *Proc. Natl. Acad. Sci. U. S. A.* **97**:6826–6831.
44. Jones, K.R., Farinas, I., Backus, C., and Reichardt, L.F. 1994. Targeted disruption of the BDNF gene perturbs brain and sensory neuron development but not motor neuron development. *Cell.* **76**:989–999.
45. Minichiello, L., and Klein, R. 1996. TrkB and TrkC neurotrophin receptors cooperate in promoting survival of hippocampal and cerebellar granule neurons. *Genes Dev.* **10**:2849–2858.
46. Xu, B., et al. 2000. Cortical degeneration in the absence of neurotrophin signaling: dendritic retraction and neuronal loss after removal of the receptor TrkB. *Neuron.* **26**:233–245.
47. Castren, E., and Tanila, H. 2006. Neurotrophins and dementia-keeping in touch. *Neuron.* **51**:1–3.
48. Dorsey, S.G., et al. 2006. In vivo restoration of physiological levels of truncated TrkB.T1 receptor rescues neuronal cell death in a trisomic mouse model. *Neuron.* **51**:21–28.
49. Salehi, A., et al. 2006. Increased App expression in a mouse model of Down's syndrome disrupts NGF transport and causes cholinergic neuron degeneration. *Neuron.* **51**:29–42.
50. Eckman, E.A., Watson, M., Marlow, L., Sambamurti, K., and Eckman, C.B. 2003. Alzheimer's disease beta-amyloid peptide is increased in mice deficient in endothelin-converting enzyme. *J. Biol. Chem.* **278**:2081–2084.
51. Melchor, J.P., Pawlak, R., and Strickland, S. 2003. The tissue plasminogen activator-plasminogen proteolytic cascade accelerates amyloid-beta (Abeta) degradation and inhibits Abeta-induced neurodegeneration. *J. Neurosci.* **23**:8867–8871.
52. Atwood, C.S., et al. 2003. Amyloid-beta: a chameleon walking in two worlds: a review of the trophic and toxic properties of amyloid-beta. *Brain Res. Brain Res. Rev.* **43**:1–16.
53. Feng, X.-H., Filvaroff, E.H., and Derynck, R. 1995. Transforming growth factor-β (TGF-β)-induced down-regulation of cyclin A expression requires a functional TGF-β receptor complex. *J. Biol. Chem.* **270**:24237–24245.
54. Gossen, M., and Bujard, H. 1992. Tight control of gene expression in mammalian cells by tetracycline-responsive promoters. *Proc. Natl. Acad. Sci. U. S. A.* **89**:5547–5551.
55. Keeton, M.R., Curriden, S.A., van Zonneveld, A.-J., and Loskutoff, D.J. 1991. Identification of regulatory sequences in the type 1 plasminogen activator inhibitor gene responsive to transforming growth factor β. *J. Biol. Chem.* **266**:23048–23052.
56. Dennler, S., et al. 1998. Direct binding of Smad3 and Smad4 to critical TGFβ-inducible elements in the promoter of human plasminogen activator inhibitor-type 1 gene. *EMBO J.* **17**:3091–3100.
57. Everall, I.P., DeTeresa, R., Terry, R., and Masliah, E. 1997. Comparison of two quantitative methods for the evaluation of neuronal number in the frontal cortex in Alzheimer disease. *J. Neuropathol. Exp. Neurol.* **56**:1202–1206.
58. Masliah, E., et al. 1992. Spectrum of human immunodeficiency virus-associated neocortical damage. *Ann. Neurol.* **32**:321–329.
59. Buttini, M., et al. 1999. Expression of human apolipoprotein E3 or E4 in the brains of *Apoe*$^{-/-}$ mice: Isoform-specific effects on neurodegeneration. *J. Neurosci.* **19**:4867–4880.
60. Chin, J., et al. 2005. Fyn kinase induces synaptic and cognitive impairments in a transgenic mouse model of Alzheimer's disease. *J. Neurosci.* **25**:9694–9703.
61. Toggas, S.M., et al. 1994. Central nervous system damage produced by expression of the HIV-1 coat protein gp120 in transgenic mice. *Nature.* **367**:188–193.
62. Masliah, E., et al. 1992. Three-dimensional analysis of the relationship between synaptic pathology and neuropil threads in Alzheimer disease. *J. Neuropathol. Exp. Neurol.* **51**:404–414.